Original Article

JCBFM

Journal of Cerebral Blood Flow & Metabolism
2019, Vol. 39(7) 1326–1335

DOI: 10.1177/0271678X18758548
journals.sagepub.com/home/jcbfm
SAGE

Cerebral perfusion and compensatory blood supply in patients with recent small subcortical infarcts

Salvatore Rudilosso[1], Carlos Laredo[1,2], Marco Mancosu[3], Nuria Moya-Planas[2], Yashu Zhao[1], Oscar Chirife[4], Ángel Chamorro[1,2] and Xabier Urra[1,2]

Abstract

Hypoperfusion is the typical perfusion pattern associated with recent small subcortical infarcts of the brain, but other perfusion patterns may be present in patients with these infarcts. Using CT perfusion, we studied 67 consecutive patients who had a small subcortical infarct at a follow-up MRI study to investigate the correlation between the perfusion pattern and the clinical and radiological course. On CT perfusion map analysis, 51 patients (76%) had focal hypoperfusion, 4 patients (6%) had hyperperfusion and the remaining 12 patients (18%) showed no abnormalities. On dynamic sequential imaging analysis obtained from the source perfusion images, 32 patients (48%) had a sustained hypoperfusion pattern, 11 patients (16%) had a reperfusion pattern, and 18 patients (27%) had a delayed compensation pattern. Systolic blood pressure was higher in patients with sustained hypoperfusion although the perfusion pattern was independent of the final volume of infarction. These results reinforce the notion that mechanisms other than hypoperfusion are at play in patients with small subcortical infarcts including the intervention of compensatory sources of blood flow. The ultimate clinical significance of these perfusion patterns remains to be determined in larger series of patients assessed longitudinally.

Keywords

Recent small subcortical infarcts, lacunar infarcts, computed tomography perfusion, reperfusion, collateral blood supply

Received 15 September 2017; Revised 5 December 2017; Accepted 9 January 2018

Introduction

Recent small subcortical infarcts (RSSIs) are the cause of up to a quarter of all ischemic strokes[1] and are defined by radiological criteria regardless etiological considerations.[2] Most of RSSIs are lacunar infarcts caused by occlusion of a single perforating artery due to lipohyalinosis,[3,4] although other pathological conditions such as microatheromas, atheromatous branch disease[5] or microembolisms[6] can also cause subcortical infarcts that are indistinguishable from "true" lacunar infarcts on brain imaging.

RSSIs can be observed as hypoperfused areas on computed tomography perfusion (CTP) maps despite their small volume.[7–12] The diagnostic yield of CTP in detecting RSSIs is conditioned by a high rate of false negative scans that have been explained by limited coverage, movements during image acquisition, bone artifacts, and low signal-to-noise ratio of the perfusion maps.[13] However, some RSSIs show no perfusion defects despite complete brain coverage and good quality of image acquisition,[7] raising the possibility that the lack of focal hypoperfusion on CTP maps could also be indicative of restored perfusion rather than a limitation of the technique. Indeed, areas of ischemic penumbra have been described in patients with subcortical infarcts,[7,14] while patients with lacunar infarcts

[1]Functional Unit of Cerebrovascular Diseases, Hospital Clínic, Barcelona, Spain
[2]Institut d'Investigacions Biomèdiques August Pi i Sunyer, Barcelona, Spain
[3]Department of Neurology, AOU Policlinico Universitario, Monserrato (Cagliari), Italy
[4]Department of Radiology, Hospital Clínic, Barcelona, Spain

Corresponding author:
Ángel Chamorro, Department of Neurology, Hospital Clinic, Villarroel 170, Barcelona 08036, Spain.
Email: achamorro@clinic.cat

and fluctuating symptoms may also exhibit fleeting perfusion abnormalities.[15]

Although the prevailing idea is that most subcortical structures are perfused by terminal branches of perforating arteries,[16] accumulating data also suggest that collateral blood flow may be relevant in the deep brain microcirculation. Thus, a recent series of patients with acute lacunar infarcts studied using dynamic angiograms generated by perfusion weighted raw images identified the presence of assorted perfusion patterns including some that could be attributed to collateral blood flow.[17] However, other possible compensatory mechanisms were not assessed because only patients with hypoperfusion in the perfusion-weighted imaging were studied. Especially in patients with RSSIs that do not show hypoperfusion, pre-occluded perforating arteries may have recanalized and thus perfusion may have been restored.

The aims of the current study were to confirm the existence of different brain perfusion patterns in patients with acute RSSIs, evaluate the utility of CTP for this purpose and assess the clinical and radiological correlates corresponding to the hemodynamic pattern. Ultimately, a better knowledge of the pathophysiology of RSSIs could lead to more effective therapeutic measures in these patients.

Methods

Patients

From a total of 798 patients evaluated in our emergency service for acute stroke reperfusion therapy from May 2011 to September 2016, 565 patients had large vessel occlusions, cortical infarcts or subcortical infarcts not classifiable as RSSIs, 103 had a hemorrhagic stroke, 38 were stroke mimics, and 18 were classified as lacunar infarcts but were not confirmed at follow-up MRI. The remaining 74 patients (9%) had an RSSI confirmed at follow-up magnetic resonance imaging (MRI), and 7 had to be excluded because of the poor quality of the perfusion maps ($n = 4$) or because there were multiple acute infarcts on the follow-up MRI ($n = 3$). We collected demographic and laboratory data, the systolic and diastolic blood pressure recorded in the emergency room, preadmission antithrombotic therapy, and whether thrombolytic therapy was given. Stroke etiology was classified using the Trial of Org 10172 in Acute Stroke Treatment (TOAST) criteria after a full diagnostic workup. Neurological impairment was assessed by the National Institutes of Health Stroke Scale (NIHSS) at admission and daily until discharge. We defined ''clinical fluctuation'' as a transient increase of more than 1 point in the NIHSS score from stroke onset to 24 h after admission, while ''neurological worsening'' referred to an increment of more than 1 point in the NIHSS score that persisted until discharge. Functional outcome was measured with the use of the modified Rankin Scale (mRS) premorbidly and at 90 days by a stroke neurologist certified in mRS. Poor outcome was defined as an mRS greater than 1 at 90 days. The study protocol was approved by the local Clinical Research Ethics Committee from Hospital Clínic of Barcelona under the requirements of Spanish legislation in the field of biomedical research, the protection of personal data (15/1999) and the standards of Good Clinical Practice, as well as with the Helsinki Declaration of 1975/1983. Patient consent was not required due to the retrospective nature of the study design and the lack of patient interaction.

Image acquisition

The multimodal brain CT study for acute stroke included a non-contrast CT (NCCT) scan, a CTP, and a CT angiography. As our local neuroimaging protocol until the end of 2011 included a second CTP study at days 2–3 after stroke, one patient in this cohort underwent two CTP acquisitions. These studies were performed at admission on a Somatom Definition Flash 128-section dual-source CT system (Siemens, Erlangen, Germany) with a 98-mm z-coverage and 26 time points acquired each 1.5 s (total acquisition time, 39 s); 50 mL of nonionic iodinated contrast was administered intravenously at 5 mL/s by using a power injector. CTP imaging parameters were 80 kV (peak), 250 mAs, 1.5 s rotation, and 2 mm thickness. CTP maps were calculated with Syngo CT Neuro Perfusion VA20 (Siemens), which uses singular-value decomposition without delay correction and automatically performs motion correction and selects an arterial input function (AIF) from an unaffected artery and venous output function from a large draining vein. We generated the following perfusion maps: cerebral blood flow (CBF), cerebral blood volume (CBV), time to peak (TTP) and time to drain (TTD).

MRI was performed on a 1.5 T scanner and included a diffusion-weighted imaging (DWI) sequence, obtained with b-values of 0 and 1000, 5-mm section thickness, and 128×128 matrix. FLAIR images were obtained with TR = 9000 ms, TE = 114 ms, FoV = 240 mm and slice thickness 5 mm.

Image postprocessing

NCCT and CT angiography. A neurologist (SR) identified on the admission NCCT scans the areas of acute low attenuation in brain tissue corresponding to hyperintense signals on the DWI-MRI performed at

follow-up. The same reader (SR) also graded the presence of atheromatosis defined as stenosis >50% of the arteries supplying the ischemic areas on CT angiography.

MRI. We defined RSSIs according to the STRIVE classification[2] as a symptomatic hyperintensity in the territory of one perforating arteriole measuring less than 20 mm in its maximum diameter in the axial plane on DWI. Small subcortical strokes due to large vessel occlusions of the main cerebral arteries were excluded from the analysis. We described the localization of RSSIs and calculated the ischemic volume with a semi-automatic segmentation of the ischemic lesion using Amira® software.

An investigator (MM) quantified the burden of chronic white matter hyperintensities using both a visual rating score (age-related white matter changes, ARWMC)[18] and a semi-automatic volumetric analysis. White matter hyperintensities on fluid attenuation inverse recovery (FLAIR) were segmented using the Amira® software. The white matter hyperintensities volume was calculated after manually excluding other hyperintensities not deemed representative of chronic white matter lesions, such as acute infarcts (confirmed on DWI), cortical hyperintensities and imaging artifacts.

CTP. The localization of the RSSIs was first identified on DWI. Whenever the TTD maps showed a well-defined area of delayed perfusion, an ROI was drawn on the TTD maps. Alternatively, an ROI was drawn on the DWI sequence and it was then shifted into the perfusion maps after co-registration. An investigator trained in CTP analysis (SR) visually evaluated the CTP maps: CBF and CBV were classified as reduced, normal or increased, whereas time maps (TTD) were classified as normal or delayed in the ROI compared with the corresponding area in the opposite hemisphere. Then, we classified a global perfusion pattern as follows: hypoperfusion (reduced CBF and delayed TTD), normoperfusion (not altered CBF and TTD) and hyperperfusion (increased CBF with normal TTD). Then we measured the absolute value of CBF, CBV and TTD inside the ROI. Global venous drainage (GVD) was defined on CTP as the time difference (seconds) between the TTP of the AIF and the TTP of the transverse venous sinus.

Dynamic 4D CT angiograms. Two technicians (CL, NMP) processed all imaging data using MATLAB (R2015b, Mathworks, Natick, MA). Before processing CTP raw images, motion correction was applied by registering the source CTP images with a rigid co-registration algorithm implemented with Statistical Parametric Mapping (SPM12, Functional Imaging Laboratory, University College London, London, UK). BAT was assessed to generate the prebolus mean image (PMI). PMI was subtracted from each time point of the source CTP data to eliminate signal intensity from anatomical structures and to visualize only the effect of contrast filling.[19,20] Data were merged across two consecutive time points to obtain the best spatial and temporal resolution to better assess contrast agent perfusion.[20] Finally, dynamic 4D CT angiograms (D4DCTA) were computed placing merged images in a loop-movie that sequentially showed the different time points of the perfusion from the BAT to the venous contrast phase. Two trained readers (SR, YZ) not blinded to CTP maps and MRI evaluated the D4DCTA individually. Three main time frames were defined: (1) from BAT + 0 s to BAT + 6 s; (2) from BAT + 7 s to BAT + 16 s; and (3) from BAT + 17 s to BAT + 25 s, and the presence or absence of contrast filling was determined for each time frame. We considered "contrast filling" as an increased contrast signal in the ROI that was visually greater than the background noisy signal, especially in the late perfusion phases due to the contrast diffusion. We assessed the interrater reliability for the evaluation of each time frame of the perfusion and in case of discrepancies a third reader (XU) assessed the case to reach a consensus. We established three D4DCTA patterns according to the hypothesis that perfusion in RSSIs is impaired by occluded independent perforating arteries (sustained hypoperfusion pattern), but also that collateral blood flow (delayed compensation pattern), and even reperfusion due to recanalization of perforating arteries (reperfusion pattern) may occur in these infarcts (Figure 1). Consequently, D4DCTA patterns were defined depending on the contrast filling the ROI in each time frame as shown in Figure 2.

Statistics

The normal distribution of all variables was assessed and quantitative variables were described as mean (SD) or median (IQR). Continuous variables were compared with Student *t*, Mann–Whitney, or Kruskal–Wallis tests as appropriate. Correlations were assessed with Spearman coefficients, and categorical variables were compared with the Fisher exact test. Interrater agreement was assessed with the kappa statistic and was interpreted following the Altman methodology.[21] The level of significance was established at a two-tailed value of P 0.05. We performed all analyses using SPSS Version 20.0 (IBM, Armonk, New York).

Results

Clinical and radiological baseline characteristics

The baseline characteristics of the 67 patients that completed the study are shown in Table 1, including

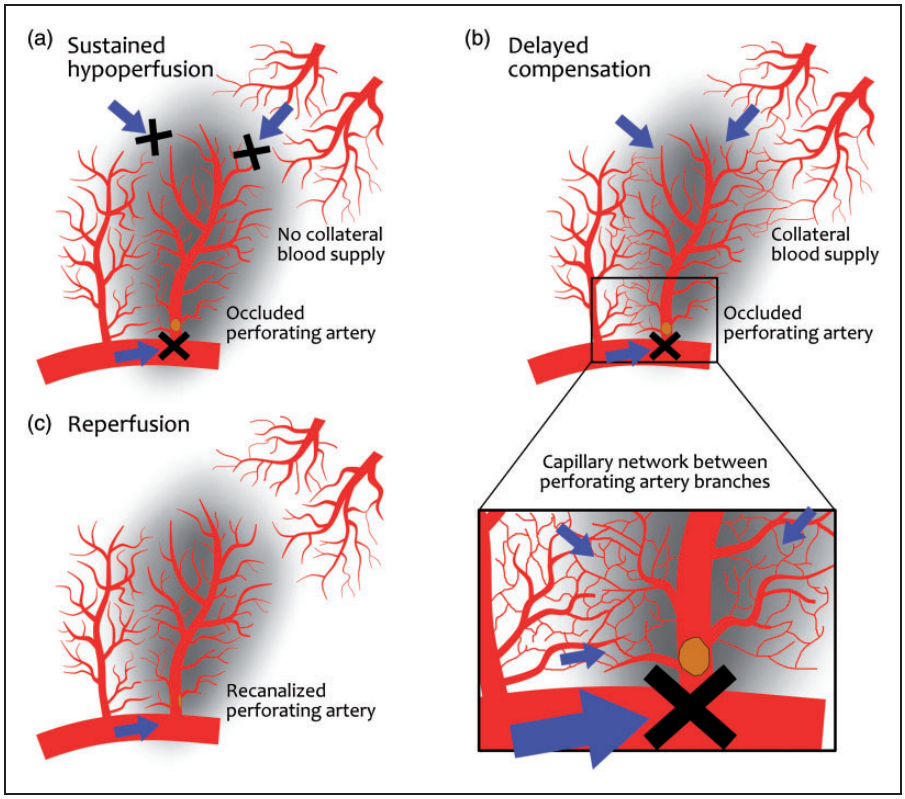

Figure 1. Hypothetic mechanisms of perfusion in RSSIs. An RSSI is shown as a smooth dark area in each figure, supplied by its own perforating artery (i.e. lenticulostriate artery) emerging from a large artery (i.e. middle cerebral artery), with a parallel perforator artery on the left and arteries from other vascular territories (i.e. large medullar arteries) above on the right. (a) Permanent occlusion in the perforator artery and no collateral blood supply by any other vascular territories, leading to a sustained hypoperfusion. (b) There is also no antegrade blood flow from the occluded artery but there are anastomoses between branches of parallel perforating arteries and arteries from other vascular territories that can enable a delayed collateral compensation. The detail shows a capillary network between branches that may vehiculate the collateral flow. (c) Reperfusion pattern in which the antegrade blood flow is restored through a patent perforating artery after recanalization of a thrombus.

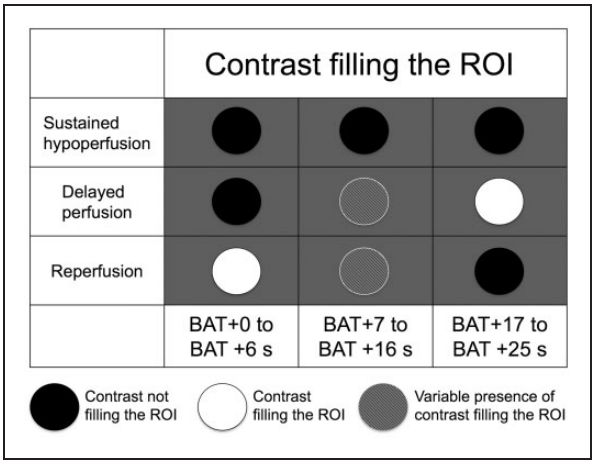

Figure 2. Schematic representation of the three pre-established perfusion patterns on dynamic 4D CT angiograms. Circles represent the ROI where the contrast filling is evaluated along the three time frames from bolus arrival time (BAT).

57 patients (85%) classified as lacunar strokes and 10 patients (15%) with coexistent atrial fibrillation or extracranial arterial stenosis. Mean systolic and diastolic blood pressure in the emergency room were 157 ± 28 mmHg and 86 ± 17 mmHg, respectively. The median time from symptom onset to CTP was 231 min (IQR, 142–325) and the median time from symptom onset to MRI was 34.2 h (IQR, 25.7–53.7). The brain structures affected by the ischemic lesion on DWI were internal capsule (37%), brainstem (25%), lenticular nucleus (19%), thalamus (17%), and centrum semiovale (2%). The median infarct volume on DWI was 0.9 cc (0.4–1.6). An acute low attenuation on the NCCT scans was observed in 14 patients (21%). Only three patients (4.5%) had focal intracranial atheromatosis in large vessels supplying the RSSIs. Patients had a median ARWMC score of 5 (2–8) and a median white matter hyperintensities on FLAIR of 44 cc (22–97), which indicate a mild burden of leukoaraiosis.[22]

Table 1. Demographic and clinical data of the study population.

Age, years, mean (SD)	66.3 (12.1)
Female gender, *n* (%)	27 (40)
Baseline NIHSS, median (IQR)	4 (3–7)
Pre-stroke mRS, median (IQR)	0 (0–0)
Clinical syndrome, *n* (%)	
Pure motor	25 (37)
Pure sensitive	1 (2)
Sensorimotor	20 (30)
Ataxia-hemiparesis	11 (16)
Others	10 (15)
Smoking habit, *n* (%)	20 (30)
Hypertension, *n* (%)	39 (58)
Diabetes mellitus, *n* (%)	15 (22)
Hyperlipidemia, *n* (%)	27 (40)
Atrial fibrillation, *n* (%)	4 (6)
Myocardial infarction, *n* (%)	3 (5)
Previous ischemic stroke, *n* (%)	7 (10)
Intravenous thrombolysis, *n* (%)	36 (53)
TOAST not lacunar, *n* (%)	10 (15)

NIHSS: National Institutes of Health Stroke Scale; mRS: modified Rankin Scale; TOAST: Trial of Org 10172 in Acute Stroke Treatment; IQR: interquartile range.

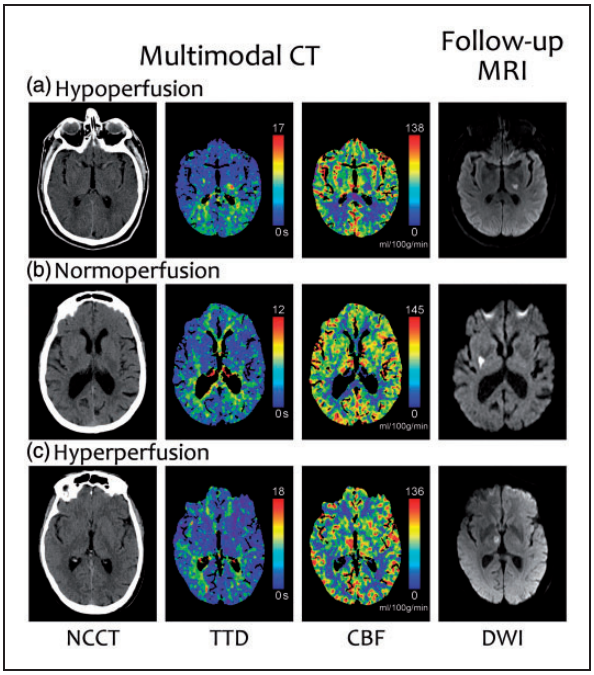

Figure 3. Three representative examples of the perfusion patterns on CTP maps. (a) Hypoperfusion: delayed TTD and low CBF. (b) Normoperfusion (normal TTD and CBF). (c) Hyperperfusion (normal TTD and high CBF). Notice that the lesion in the second row is not identifiable in the CTP maps, despite the good quality of the image and the absence of bone artifacts.

CTP maps

On visual inspection, hypoperfusion on CTP was identified in 51 patients (76%), perfusion was normal in 12 patients (18%) and hyperperfusion was observed in the remaining 4 patients (6%) (Figure 3). CBF and CBV values in the ROI were higher in patients with hyperperfusion, while TTD was longer in patients with hypoperfusion. The infarct volume on DWI and time from stroke onset to CTP acquisition did not differ between CTP groups. Patients with hyperperfusion or without perfusion abnormalities were more likely to show an acute low attenuation at the baseline NCCT (Table 2). A single patient with two CTP acquisitions showed at first exam hypoperfusion in the right putamen without signs of acute ischemia on NCCT, while a second CTP performed 48 h later showed no abnormalities and an established putaminal infarct on NCCT (Suppl. Figure).

Dynamic 4D computed tomography angiograms

The most frequent D4DCTA pattern was sustained hypoperfusion, occurring in 32 patients (48%), followed by delayed perfusion in 18 patients (27%) and reperfusion in 11 patients (16%) (Figure 4). The remaining six patients (9%) were not classifiable for poor quality of the images on D4DCTA and were excluded from the analysis. Inter-rater agreement between the two observers was good for the three time frames evaluated (from BAT + 0 s to BAT + 6 s, kappa 0.80; from BAT + 7 s to BAT + 16 s, kappa 0.70; from BAT + 17 s to BAT + 25 s, kappa 0.64). Unlike any of the 11 patients with reperfusion on D4DCTA, 31 of 32 patients with sustained hypoperfusion on D4DCTA (97%) and 16 of 18 patients with delayed compensation on D4DCTA (89%) had hypoperfusion pattern on CTP maps (Suppl. Table). Expectedly, as shown in Table 3, CBF was similar in patients with sustained hypoperfusion and delayed compensation patterns, and higher in patients with reperfusion pattern. TTD was shorter in patients with reperfusion compared to the others patients. The sequential images on D4DCTA showed that contrast filling was centripetal in patients with delayed perfusion pattern and antegrade in patients with reperfusion pattern, and how contrast filling and washout presented earlier in patients with reperfusion pattern (Suppl. Video).

Systolic blood pressure was highest in patients with sustained hypoperfusion and there were no differences in diastolic blood pressure between the D4DCTA pattern groups. Time from stroke onset to CTP acquisition was higher in patients with reperfusion pattern (median 212 min, IQR 120–308) compared to the other patterns (median 274 min, IQR 216–535), but the difference was

Table 2. Radiological results in the three CTP map groups.

	Hypoperfusion (N = 51)	Normoperfusion (N = 12)	Hyperperfusion (N = 4)	*p*
CBF, mL/100 g/min, mean (SD)	26.8 (10.0)	42.2 (15.3)	85.9 (21.2)	<0.005
CBV, mL/100 g, mean (SD)	3.0 (0.8)	3.1 (0.6)	4.7 (1.0)	0.017
TTD, s, mean (SD)	9.0 (3.4)	5.4 (2.0)	2.9 (0.5)	0.001
Time to CTP, min, median (IQR)	225 (142–313)	253 (108–489)	264 (109–541)	0.367
Low attenuation on NCCT, *n* (%)	6 (11.8)	5 (41.7)	3 (75)	0.002
Infarct volume on DWI, cc, median (IQR)	0.9 (0.5–1.6)	0.6 (0.3–1.6)	0.9 (0.8–1.0)	0.915
GVD, s, median (IQR)	6 (6–7)	7 (6–7)	6 (6–6.5)	0.881

CBF: cerebral blood flow; CBV: cerebral blood volume; TTD: time to drain; CTP: computed tomography perfusion; NCCT: non-contrast computed tomography; DWI: diffusion-weighted imaging; GVD: global venous drainage; IQR: interquartile range: SD: standard deviation.

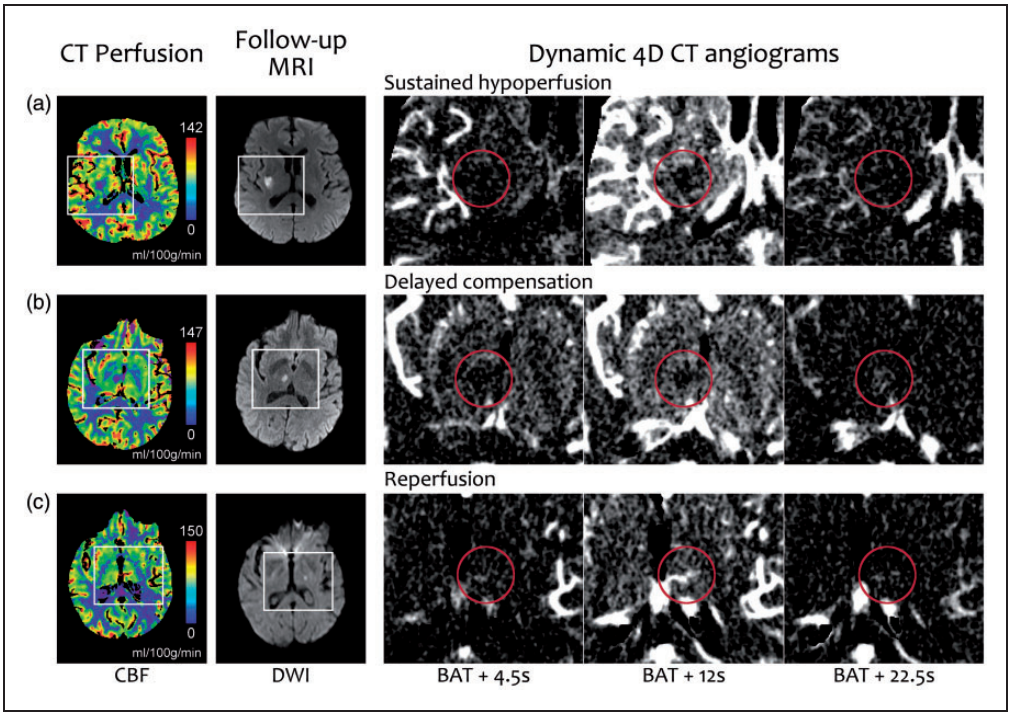

Figure 4. Representative examples of each of the three commonest perfusion patterns on dynamic 4D CT angiograms (D4DCTA). The first and second columns show the CBF map and DWI, with white rectangles marking the areas enlarged in the next three columns that show frames of the D4DCTA with different times from the bolus arrival time (BAT). The red circle indicates the ROI of the ischemic lesion. (a) There is no contrast filling the ROI in any frame, which is consistent with a sustained hypoperfusion. The signal in the ROI in the third frame is not higher than in the surrounding parenchyma. (b)There is a late contrast filling visible in the third frame, indicating a delayed compensation. (c)An early antegrade contrast filling is visible in the first frame, consistent with reperfusion. For a better understanding of these patterns, see the Supplemental video online.

marginally significant ($p = 0.064$). The presence of low attenuation on NCCT was highest in patients with reperfusion pattern and lowest in patients with sustained hypoperfusion. The DWI volume of infarction, the grade of leukoaraiosis and the GBV did not differ between the D4DCTA groups (Table 3).

Discussion

The results of this study confirmed that different perfusion patterns are identifiable by D4DCTA in patients with RSSIs. Notably, more than one-third of the patients did harbor delayed perfusion or reperfusion

Table 3. Main clinical and radiological results in the three D4DCTA pattern groups.

	Sustained hypoperfusion (N = 32)	Delayed compensation (N = 18)	Reperfusion (N = 11)	*p*
Smoking, *n* (%)	10 (31)	6 (33)	1 (9)	0.304
Hypertension, *n* (%)	18 (56)	9 (50)	7 (64)	0.770
Diabetes mellitus, *n* (%)	8 (25)	2 (11)	3 (27)	0.414
Hyperlipidemia, *n* (%)	11 (34)	6 (33)	7 (64)	0.190
Intravenous thrombolysis, *n* (%)	16 (50)	11 (61)	8 (73)	0.392
Baseline NIHSS, median (IQR)	4 (3–7)	4.5 (3–7)	4 (4–10)	0.434
SBP at admission, mmHg, mean (SD)	168 (27)	149 (20)	146 (28)	0.010
DBP at admission, mmHg, mean (SD)	89 (16)	84 (20)	81 (18)	0.365
Glucose, mg/dL, mean (SD)	141 (54)	129 (41)	133 (39)	0.713
Fluctuating symptoms, *n* (%)	21 (34)	24 (39)	33 (55)	0.497
Neurological worsening, *n* (%)	6 (9)	10 (17)	6 (9)	0.712
mRS score > 1 at 90 days, *n* (%)	32 (53)	17 (27)	22 (36)	0.198
Low attenuations on NCCT, *n* (%)	6 (9)	14 (22)	28 (45)	0.033
Infarct volume on DWI, cc, median (IQR)	0.9 (0.5–1.6)	0.8 (0.4–1.8)	0.9 (0.3–2.1)	0.963
Time to CTP, minutes, median (IQR)	225 (122–322)	166 (113–247)	274 (216–535)	0.101
WMH volume on FLAIR, cc, median (IQR)	3.2 (1.4–11.3)	5.0 (1.9–14.1)	5.1 (1.7–8.4)	0.494
CBF, mL/100 g/min, mean (SD)	29.5 (13.7)	26.1 (11.3)	57 (27.5)	<0.001
CBV, mL/100 g, mean (SD)	3.2 (0.8)	2.8 (0.5)	3.7 (1.0)	0.17
TTD, s, mean (SD)	8.6 (3.7)	8.8 (2.7)	4.5 (2.3)	0.001
GVD, s, median (IQR)	6 (6–6.8)	6 (5–7)	6.5 (6–7)	0.645

NHISS: National institute of Health Stroke Scale; mRS: modified Rankin Scale; SBP: systolic blood pressure; DBP: diastolic blood pressure; NCCT: non-contrast computed tomography; DWI: diffusion-weighted imaging; CTP: computed tomography perfusion; FLAIR: fluid attenuated inverse recovery; WMH: white matter hyperintensities; CBF: cerebral blood flow; CBV: cerebral blood volume: TTD: time to drain; GVD: global venous drainage; IQR: interquartile range: SD: standard deviation.

patterns strongly supportive of the existence of compensatory hemodynamic mechanisms.

Hypoperfusion on CTP maps was confirmed to be the most frequent finding in patients with RSSIs, but perfusion could also appear normal or even increased. Hyperperfusion is a phenomenon that may occur in large vessel stroke after recanalization,[23] but was anecdotally described in small cortical strokes[24] and in lacunar infarcts.[17] The presence of an established brain infarction on NCCT at the time of CTP acquisition was paradoxically less frequent in patients with hypoperfusion on CTP maps compared to those with normo-hyperperfusion. Thus, it is possible that changes in perfusion in RSSIs are time-dependent, and hypoperfusion may represent the first mechanism occurring after a perforating artery occlusion that could be followed by increased CBF associated with irreversible ischemia. Although time from symptom onset to CTP did not significantly differ between the CTP map groups in this cohort, it is possible that patients with normal or increased perfusion on CTP maps could have shown hypoperfusion had the imaging been acquired earlier. In fact, the only patient who had two perfusion studies over time showed that this course of events did not prevent the appearance of a full ischemic infarction on later imaging. However, longitudinal studies with repeated imaging are warranted to confirm that perfusion pattern may change over time in patients with RSSIs.

In almost half part of the patients of this cohort, the perfusion in the ischemic area was absent during the entire acquisition of the perfusion study on D4DCTA. This pattern of sustained hypoperfusion is consistent with the permanent occlusion of one arteriole in a terminal vascular territory that does not receive any other vascular supply and loses its self-regulation capacity.[16] Systolic blood pressure at admission was higher in these patients compared to patients with other perfusion patterns. Hypertension is common in acute stroke, especially in lacunar infarcts,[25] and in large vessel stroke, blood pressure remains elevated in patients that do not achieve recanalization compared to those who receive intra-arterial thrombolysis.[26] Therefore, the sustained hypoperfusion pattern in

RSSIs could represent a similar condition where elevated blood pressure may help to increase perfusion in presence of a persistent vessel occlusion without sufficient collateral blood flow.

One-quarter of the patients showed a delayed contrast filling after the initial lack of perfusion. This pattern of delayed perfusion could be the result of either slow perfusion throughout a dilated vessel proximally narrowed by a sub-occlusive thrombus, or blood flow from collateral vessels. Animal models demonstrated that vasodilatation of the perforating arteries is more efficient than the flow provided by pial vessels and this mechanism could play a compensatory role in territories with poor collateral supply.[27,28] Nevertheless, the late contrast enhancement reminds collateral blood supply in large vessel stroke[29] and in patients with acute subcortical strokes in moyamoya disease,[30] a condition characterized by capillary sprouting and anastomosis formation among deep perforating arteries. In healthy subjects, perforating arteries have several degrees of ramifications and macroscopic anastomoses are common in their extra-parenchymal portions.[31] Some microscopy studies showed few connections between perforating branches and poor capillary network in both basal ganglia and cerebral white matter,[32–35] while in vivo perfusion staining studies in mice showed a wide capillary network in the deep grey matter.[36,37] Overall, perforating arteries are considered as functionally independent vessels,[38] but this hypothesis should be reconsidered in light of new evidences from radiological studies in humans and in animal models.

Patients with hyperperfusion and more than half of those with normoperfusion on CTP maps showed a reperfusion pattern in the D4DCTA analysis, characterized by an early contrast filling and highest CBF values. Although perforating arteries were not directly visible with this technique, the contrast filled the ROI in an antegrade way, which is consistent with recanalization of the previously occluded arteriole and maximal dilatation. The reperfusion pattern in D4DCTA supports the hypothesis that some RSSIs may have an embolic source, as Fisher already described in about 10% of patients with lacunes without occlusion in the feeding perforating artery.[39] In this cohort, reperfusion was associated with low attenuation in the NCCT scans compared to the other patterns in D4DCTA, but final stroke volume was not different between groups. Therefore, reperfusion may have occurred in an already established ischemic parenchyma in a perforating arteriole with impaired autoregulation, and reperfusion may have been futile or even harmful for the ischemic tissue.[40]

As perforating arteries are not directly visible with D4DCTA, the findings observed on both patients with delayed compensation and reperfusion may be also due to an increased permeability of the blood–brain barrier and contrast extravasation through the ischemic tissue. In fact, pro-inflammatory cytokines[41] and excitotoxic GABA/glutamate imbalance are common in lacunar infarcts,[42] and blood–brain barrier may be damaged in these infarcts.[43] In case of leakage of the capillary wall, enhancement is a late phenomenon due to a progressive accumulation of contrast into the interstitial space.[44] Contrarily, contrast washed out quickly in patients with reperfusion pattern and also decreased in the last sequences of the D4DCTA in patients with delayed compensation. Thus, it seems unlikely that blood–brain barrier permeability is the main responsible for these perfusion patterns.

The venous compartment is related to collateral blood flow and could be involved in the hemodynamics of RSSIs.[45] In this cohort, there were no differences in the GVD between patients with different perfusion patterns, but local flow abnormalities in veins supplying RSSIs may be present and should be assessed in the future by more detailed dynamic angiography studies.

Leukoaraiosis is related to brain hypoperfusion[46] but its relationship with collateral blood flow is controversial in stroke.[47,48] In our study, we did not find greater leukoaraiosis in patients with delayed compensation compared to the rest of groups, but our analysis included a relatively young group with a low prevalence of leukoaraiosis.

Among the perfusion patterns in D4DCTA, we did not find any significant correlations with functional outcome, clinical fluctuations or neurological worsening. However, the hemodynamics in the perforating arteries may change longitudinally during the ischemic process and it cannot be ruled out that the images acquired at admission anticipated a later hemodynamic process that lead to the typical fluctuations of lacunar infarcts described as ''capsular warning.''[49]

Our study has several limitations that caution the interpretation of the results. Particularly, we included a small cohort of patients that had perfusion studies acquired because they were potential candidates for acute revascularization therapies. As a result, patients arriving late to medical attention or those presenting with only mild o transient symptoms were not included in the study. This may have underestimated the protective role of reperfusion and collateral blood flow in patients with RSSIs, since only patients with permanent infarcts on brain MRI were included in the study. Unfortunately, repeating perfusion studies systematically would imply safety concerns due to excessive radiation and contrast toxicity.[50]

In conclusion, this study confirmed that the sequential analysis of the perfusion images on CT is able to identify different perfusion patterns in RSSIs.

Hypoperfusion was the most frequent finding, and was associated with higher systolic blood pressure. We also confirmed the presence of a delayed compensation in some patients that may imply collateral blood flow, vasodilatation or other still unknown mechanisms. Finally, those patients with RSSIs that did not show the typical hypoperfused pattern in CTP maps, could represent those experiencing a reperfusion phenomenon resulting from recanalization of perforating artery, rather than a limitation of the technique. Future research should investigate the clinical significance of reperfusion and the function of micro-collateral networks in subcortical infarcts, and whether they may represent a therapeutic target.

Funding

The author(s) received no financial support for the research, authorship, and/or publication of this article.

Acknowledgements

Yashu Zhao received a scholarship from China Scholarship Council (CSC).

Declaration of conflicting interests

The author(s) declared no potential conflicts of interest with respect to the research, authorship, and/or publication of this article.

Authors' contributions

Conception and design of study: Salvatore Rudilosso, Xabier Urra.
Acquisition of data: Salvatore Rudilosso, Oscar Chirife, Marco Mancosu, Nuria Moya-Planas, Yashu Zhao.
Analysis and/or interpretation of data: Salvatore Rudilosso, Xabier Urra, Carlos Laredo.
Drafting the manuscript: Salvatore Rudilosso.
Revising the manuscript critically for important intellectual content: Ángel Chamorro, Xabier Urra.
Approval of the version of the manuscript to be published: Salvatore Rudilosso, Carlos Laredo, Marco Mancosu, Nuria Moya-Planas, Yashu Zhao, Oscar Chirife, Ángel Chamorro, Xabier Urra.

Supplementary material

Supplementary material for this paper can be found at the journal website: http://journals.sagepub.com/home/jcb

References

1. Sudlow CLM and Warlow CP. Comparable studies of the incidence of stroke and its pathological types: results from an international collaboration. *Stroke* 1997; 28: 491–499.
2. Wardlaw JM, Smith EE, Biessels GJ, et al. Neuroimaging standards for research into small vessel disease and its contribution to ageing and neurodegeneration. *Lancet Neurol* 2013; 12: 822–838.
3. Fisher CM. Lacunar strokes and infarcts: a review. *Neurology* 1982; 32: 871–876.
4. Fisher CM. The arterial lesions underlying lacunes. *Neurology* 1965; 15: 774–784.
5. Petrone L, Nannoni S, Del Bene A, et al. Branch atheromatous disease: a clinically meaningful, yet unproven concept. *Cerebrovasc Dis* 2016; 41: 87–95.
6. Arboix A and Martí-Vilalta JL. New concepts in lacunar stroke etiology: the constellation of small-vessel arterial disease. *Cerebrovasc Dis* 2004; 17: 58–62.
7. Rudilosso S, Urra X, San Román L, et al. Perfusion deficits and mismatch in patients with acute lacunar infarcts studied with whole-brain CT perfusion. *Am J Neuroradiol* 2015; 36: 1407–1412.
8. Das T, Settecase F, Boulos M, et al. Multimodal CT provides improved performance for lacunar infarct detection. *Am J Neuroradiol* 2015; 36: 1069–1075.
9. Benson JC, Payabvash S, Mortazavi S, et al. CT perfusion in acute lacunar stroke: detection capabilities based on infarct location. *Am J Neuroradiol* 2016; 37: 2239–2244.
10. Yang J, d'Esterre C, Ceruti S, et al. Temporal changes in blood-brain barrier permeability and cerebral perfusion in lacunar/subcortical ischemic stroke. *BMC Neurol* 2015; 15: 214.
11. Cao W, Yassi N, Sharma G, et al. Diagnosing acute lacunar infarction using CT perfusion. *J Clin Neurosci* 2016; 29: 70–72.
12. Tan MY, Singhal S, Ma M, et al. Examining subcortical infarcts in the era of acute multimodality CT imaging. *Front Neurol* 2016; 7: 220.
13. Monelli N, Rota E, Micheletti E, et al. The ''vexata quaestio'' on lacunar stroke: the role of CT perfusion imaging. *Am J Neuroradiol* 2017; 38: 11–12.
14. Förster A, Kerl HU, Wenz H, et al. Diffusion- and perfusion-weighted imaging in acute lacunar infarction: is there a mismatch? *PLoS One* 2013; 8: 77428.
15. Rudilosso S, Urra X, Chirife O, et al. Altered brain computed tomography perfusion in patients with fluctuating lacunar syndrome and normal magnetic resonance imaging. *JAMA Neurol* 2016; 73: 348–349.
16. Mohr JP. Lacunes. *Stroke* 1982; 13: 3–11.
17. Förster A, Mürle B, Böhme J, et al. Perfusion-weighted imaging and dynamic 4D angiograms for the estimation of collateral blood flow in lacunar infarction. *J Cereb Blood Flow Metab* 2016; 36: 1744–1754.
18. Wahlund LO, Barkhof F, Fazekas F, et al. A new rating scale for age-related white matter changes applicable to MRI and CT. *Stroke* 2001; 32: 1318–1322.
19. Campbell BC, Christensen S, Tress BM, et al. Failure of collateral blood flow is associated with infarct growth in ischemic stroke. *J Cereb Blood Flow Metab* 2013; 33: 1168–1172.
20. Kim SJ, Son JP, Ryoo S, et al. A novel magnetic resonance imaging approach to collateral flow imaging in ischemic stroke. *Ann Neurol* 2014; 76: 356–369.
21. Altman DG and Bland JM. *Practical statistics for medical research*. London: Chapman and Hall, 1991.
22. Huynh TJ, Murphy B, Pettersen JA, et al. CT perfusion quantification of small-vessel ischemic severity. *Am J Neuroradiol* 2008; 29: 1831–1836.

23. Shahi V, Fugate JE, Kallmes DF, et al. Early basal ganglia hyperperfusion on CT perfusion in acute ischemic stroke: a marker of irreversible damage? *Am J Neuroradiol* 2014; 35: 1688–1692.
24. Rudilosso S, Laredo C, Urra X, et al. Different perfusion patterns in a patient with acute ischemic stroke. *J Stroke Cerebrovasc Dis* 2017; 26: 83–84.
25. Chamorro A, Sacco RL, Mohr JP, et al. Clinical-computed tomographic correlations of lacunar infarction in the Stroke Data Bank. *Stroke* 1991; 22: 175–181.
26. Mattle HP, Kappeler L, Arnold M, et al. Blood pressure and vessel recanalization in the first hours after ischemic stroke. *Stroke* 2005; 36: 264–268.
27. Yoshino H, Sakurai T, Oizumi XS, et al. Dilation of perforating arteries in rat brain in response to systemic hypotension is more sensitive and pronounced than that of pial arterioles: simultaneous visualization of perforating and cortical vessels by in-vivo microangiography. *Microvasc Res* 2009; 77: 230–233.
28. Morishita A, Kondoh T, Sakurai T, et al. Quantification of distension in rat cerebral perforating arteries. *Neuroreport* 2006; 17: 1549–1553.
29. Van Den Wijngaard IR, Holswilder G, et al. Assessment of collateral status by dynamic CT angiography in acute MCA stroke: timing of acquisition and relationship with final infarct volume. *Am J Neuroradiol* 2016; 37: 1231–1236.
30. Kim DY, Son JP, Yeon JY, et al. Infarct pattern and collateral status in adult moyamoya disease: a multimodal magnetic resonance imaging study. *Stroke* 2017; 48: 111–116.
31. Djulejić V, Marinković S, Milić V, et al. Common features of the cerebral perforating arteries and their clinical significance. *Acta Neurochir* 2015; 157: 743–754.
32. Feekes JA, Hsu SW, Chaloupka JC, et al. Tertiary microvascular territories define lacunar infarcts in the basal ganglia. *Ann Neurol* 2005; 58: 18–30.
33. Feekes JA and Cassell MD. The vascular supply of the functional compartments of the human striatum. *Brain* 2006; 129: 2189–2201.
34. Nonaka H, Akima M, Hatori T, et al. Microvasculature of the human cerebral white matter: arteries of the deep white matter. *Neuropathology* 2003; 23: 111–118.
35. Reina-De La Torre F, Rodriguez-Baeza A and Sahuquillo-Barris J. Morphological characteristics and distribution pattern of the arterial vessels in human cerebral cortex: a scanning electron microscope study. *Anat Rec* 1998; 251: 87–96.
36. Xue S, Gong H, Jiang T, et al. Indian-ink perfusion based method for reconstructing continuous vascular networks in whole mouse brain. *PLoS One* 2014; 9: 88067.
37. Lugo-Hernandez E, Squire A, Hagemann N, et al. 3D visualization and cuantification of microvessels in the whole ischemic mouse brain using solvent-based clearing and light sheet microscopy. *J Cereb Blood Flow Metab* 2017; 37: 3355–3367.
38. Moody DM, Bell MA and Challa VR. Features of the cerebral vascular pattern that predict vulnerability to perfusion or oxygenation deficiency: an anatomic study. *Am J Neuroradiol* 1990; 11: 431–439.
39. Fisher CM. Lacunar infarcts – a review. *Cerebrovasc Dis* 1991; 1: 311–320.
40. Shahi V, Fugate JE, Kallmes DF, et al. Early basal ganglia hyperperfusion on CT perfusion in acute ischemic stroke: a marker of irreversible damage? *Am J Neuroradiol* 2014; 35: 1688–1692.
41. Castellanos M, Castillo J, García MM, et al. Inflammation-mediated damage in progressing lacunar infarctions: a potential therapeutic target. *Stroke* 2002; 33: 982–987.
42. Serena J, Leira R, Castillo J, et al. Neurological deterioration in acute lacunar infarctions: the role of excitatory and inhibitory neurotransmitters. *Stroke* 2001; 32: 1154–1161.
43. Wardlaw JM, Doubal F, Armitage P, et al. Lacunar stroke is associated with diffuse blood-brain barrier dysfunction. *Ann Neurol* 2009; 65: 194–202.
44. Cuenod CA and Balvay D. Perfusion and vascular permeability: basic concepts and measurement in DCE-CT and DCE-MRI. *Diagn Interv Imaging* 2013; 94: 1187–1204.
45. Munuera J, Blasco G, Hernández-Pérez M, et al. Venous imaging-based biomarkers in acute ischaemic stroke. *J Neurol Neurosurg Psychiatry* 2017; 88: 62–69.
46. O'Sullivan M, Lythgoe DJ, Pereira AC, et al. Patterns of cerebral blood flow reduction in patients with ischemic leukoaraiosis. *Neurology* 2002; 59: 321–326.
47. Sanossian N, Ovbiagele B, Saver JL, et al. Leukoaraiosis and collaterals in acute ischemic stroke. *J Neuroimaging* 2011; 21: 232–235.
48. Giurgiutiu DV, Yoo AJ, Fitzpatrick K, et al. Severity of leukoaraiosis, leptomeningeal collaterals, and clinical outcomes after intra-arterial therapy in patients with acute ischemic stroke. *J Neurointerv Surg* 2015; 7: 326–330.
49. Donnan GA, O'Malley RN, Quang L, et al. The capsular warning syndrome: pathogenesis and clinical features. *Neurology* 1993; 43: 957–962.
50. Brix G, Lechel U, Nekolla E, et al. Estimation of radiation exposure for brain perfusion CT: standard protocol compared with deviations in protocol. *Eur J Radiol* 2015; 84: 2347–2358.